Cellular and Molecular Life Sciences (2019) 76:4355–4368
https://doi.org/10.1007/s00018-019-03116-2

ORIGINAL ARTICLE

KIF2A characterization after spinal cord injury

Oscar Seira[1,2] · Jie Liu[1] · Peggy Assinck[1,3,5] · Matt Ramer[1,2] · Wolfram Tetzlaff[1,2,4]

Received: 11 October 2018 / Revised: 5 April 2019 / Accepted: 24 April 2019 / Published online: 30 April 2019

Abstract

Axons in the central nervous system (CNS) typically fail to regenerate after injury. This failure is multi-factorial and caused in part by disruption of the axonal cytoskeleton. The cytoskeleton, in particular microtubules (MT), plays a critical role in axonal transport and axon growth during development. In this regard, members of the kinesin superfamily of proteins (KIFs) regulate the extension of primary axons toward their targets and control the growth of collateral branches. KIF2A negatively regulates axon growth through MT depolymerization. Using three different injury models to induce SCI in adult rats, we examined the temporal and cellular expression of KIF2A in the injured spinal cord. We observed a progressive increase of KIF2A expression with maximal levels at 10 days to 8 weeks post-injury as determined by Western blot analysis. KIF2A immunoreactivity was present in axons, spinal neurons and mature oligodendrocytes adjacent to the injury site. Results from the present study suggest that KIF2A at the injured axonal tips may contribute to neurite outgrowth inhibition after injury, and that its increased expression in inhibitory spinal neurons adjacent to the injury site might contribute to an intrinsic wiring-control mechanism associated with neuropathic pain. Further studies will determine whether KIF2A may be a potential target for the development of regeneration-promoting or pain-preventing therapies.

Keywords Kinesin · Cytoskeleton · Spinal cord injury · Regeneration · Neuropathic pain

Introduction

The neuronal cytoskeleton is complex and has a highly compartmentalized organization underlying the maintenance of neuronal structure [34]. It is composed of microtubules (MT), actin and neurofilaments. In addition to their role as a structural scaffold, MTs play a major role in axon growth and growth cone dynamics [25, 32–34, 40, 64]. MT dynamics are regulated by microtubule-associated proteins (MAP) [40] that are regulated by kinases, such as GSK3β, PKC and MT affinity regulating kinases (MARK), and by motor proteins [11, 14, 24, 35, 66].

Motor proteins are essential for cytoskeletal dynamics [21, 27, 64, 70]. These proteins mediate directional intracellular transport, which is fundamental for axonal regeneration and wiring after injury, and for reciprocal growth cone/cell body communication [13, 62]. There are three main motor protein superfamilies identified: kinesins, dyneins and myosins [28, 68]. Kinesins use MTs to transport cargo, although some kinesins members such as KIF2A have other roles such as mediating MT depolymerization associated with inhibition of axonal regeneration [6, 29].

KIF2A is expressed in postmitotic cells [48, 54] and its functions in the central nervous system (CNS) are poorly understood. KIF2A plays a role in determining axonal length and controls collateral branching in neurons in vitro and in vivo [30, 31, 53]. KIF2A knockout mice show aberrant brain development [30], mossy fiber sprouting and dentate

Electronic supplementary material The online version of this article (https://doi.org/10.1007/s00018-019-03116-2) contains supplementary material, which is available to authorized users.

✉ Oscar Seira
oseira.icord@gmail.com

1 International Collaboration on Repair Discoveries (ICORD), Blusson Spinal Cord Centre, University of British Columbia (UBC), 818 West 10th Avenue, Vancouver, BC V5Z 1M9, Canada

2 Department of Zoology, University of British Columbia (UBC), Vancouver, Canada

3 Graduate Program in Neuroscience, University of British Columbia (UBC), Vancouver, Canada

4 Department of Surgery, University of British Columbia (UBC), Vancouver, Canada

5 Present Address: MRC Centre for Regenerative Medicine, The University of Edinburgh, Edinburgh, UK

granule cells dendro-axonal conversion [31], and delayed axonal degeneration during pruning [43]. Nevertheless, very little is known about the expression pattern of kinesin family members in the intact or injured spinal cord. Thus, KLP4, a kinesin-like protein in *C. elegans*, is expressed in interneurons of the nerve cord where it plays a role in decreasing anterograde axonal transport [47] while KIF3B, for example, shows increased expression in microglia and astrocytes of rat spinal cords after acute injury [73].

Here, we have investigated the expression and distribution of KIF2A in the spinal cord after injury. Our findings suggest that KIF2A may be involved in axonal growth inhibition and it may play a role in the control of neuropathic pain and spasticity.

Materials and methods

SCI

Adult male Sprague–Dawley rats ($n=31$) (Charles River Laboratories, Wilmington, MA, USA) were used (DLF crush, $n=15$ (western blot), $n=4$ (histology); T9 midline contusion, $n=3$; C5 hemicontusion, $n=3$ (cross-sections), $n=3$ (longitudinal sections); non-injured, $n=3$). A dorsolateral funiculus (DLF) crush (cervical level C4/C5) was performed as previously described in our group [67]. In a second and third type of injury, the dorsal spinal column was exposed at the C4–C6 and T8–T10 vertebrae, and the lamina of C5 or T9 removed with a pair of rongeurs for the contusion models. A standardized hemicontusion or midline contusion (150 and 200 kDyn, respectively) was performed using an Infinite Horizon Impactor (Precision Systems & Instrumentation, Lexington, KY, USA). All experimental procedures used in this work were approved by the Animal Care Committee of the University of British Columbia in accordance with the guidelines of the Canadian Council on Animal Care.

In vitro cell culture, KIF2A knockdown and immunocytochemistry

Cortical neurons from C57BL/6 P0–P2 mouse pups were dissociated by combined trypsinization. Cells were placed in 24-well tissue culture dishes (Nunc, Roskilde, Denmark) on coated coverslips and grown for 48 h in Neurobasal A medium supplemented with N2 and B27. Cultures were then fixed with PFA 4% and blocked with 2% fetal bovine serum (FBS) before primary antibodies incubation (overnight at 4C). The following antibodies were used: rabbit anti-KIF2A (1:1000; Abcam, Cambridge, MA, USA) and β-III-tubulin (1:10,000; Covance). The cover slides were mounted in Fluoromount™ (Vector Labs, Burlingame, CA, USA) and analyzed with a confocal microscope (TCS SPII, Leica, Bannockburn, IL, USA). For the knockdown experiments, a siRNA duplex siRNA-KIF2A (5′-ACAACAGAA UGGUAGCGUUUCAGAT-3′, 3′-CGUGUUGUCUUA CCAUCGCAAAGUCUA-5′) plus a scrambled siRNA as a negative control were synthesized by Integrated DNA Technologies (Coralville, Iowa). In preliminary experiments, three chemically synthesized siRNAs duplexes were screened for knockdown potency using lipid nanoparticles (LNPs, Precision Nanosystems) by immunoblotting in culture (Supplementary Figure 1). The most potent duplex was then used to perform a morphological analysis of neurite outgrowth. Neurons were grown for 2 days in vitro, then transfected. Three days post-transfection neurons were fixed with PFA 4% and then immunostained following the same protocol described above. The cultures were stained with β-III-tubulin (1:10,000; Covance). All LNPs formulation was performed by Precision Nanosystems Inc. Vancouver, Canada. All morphological quantifications (axonal and collateral lengths, and total number of branches) were performed using NeuronJ [45].

Tissue processing and immunohistochemistry

The rats were perfused transcardially with PBS, followed by PFA 4%. The harvested spinal cords (DLF crush, 10 DPI; C5 hemicontusion and T9 contusion, 8 wpi) were post-fixed for 12–24 h and cryoprotected in a PBS-30% sucrose solution. The cords were subsequently snap frozen in tissue freezing media for cryostat cryosectioning (20 µm section thickness). A full set of sections of each harvested cord was stained for each animal (200 µm between sections). After thawing the sections, the following primary antibodies were used directed against: CC1 (Millipore) (1:1000), PDGFRα and PDGRβ (R&D Systems) (1:500), β-III-tubulin (1:10,000) (Covance), NeuN (Millipore) (1:500), parvalbumin (Millipore) (1:300), NF200 (1:500), PKCγ (Santa Cruz) (1:200), CD45 (BD Pharmingen) (1:300), Iba-1 (Novus Biologicals) (1:500), Chat1 (Chemicon) (1:300), calbindin (Millipore) 1:300) and GFAP (Santa Cruz) (1:300). These were applied overnight at room temperature. Secondary antibodies (1:500, Jackson) conjugated to DyLight 594, 488 and 647, respectively, were applied for 2 h at room temperature. Digital images were captured with an Imager M2 microscope (Zeiss, Jena, Germany).

Quantitative image analysis

For the stereological evaluation of the number of $KIF2A^+$ cells in the C5 cervical hemicontusion sections, cells were counted using Imager M2 microscope (Zeiss, Jena, Germany). Cell counting was performed using one set of the ten serial slides (inter-section interval in one slide was 200 µm).

On one slide, every section was used for quantification. All KIF2A$^+$ cells present in the gray matter of the ipsilateral side (injured) of the cord were counted. No KIF2A$^+$ cells were observed in any sections in the contralateral side of the cord. A total of three animals were used for quantification. For the evaluation of the percentage of KIF2A$^+$ cells, Parv$^+$ or Calb$^+$ in the DLF crush sections, randomized images from different fields (rostral and caudal) were taken at the vicinities of the injury in the gray matter where the KIF2A$^+$ cells were located (800–1000 µm, rostral and caudal). Actual counting was performed using 40× magnification. A total of four animals were used for quantification and three sections were chosen for each animal. Nine regions of interest were captured and quantified.

Protein extraction and western blot

5-mm-long segments centered at the injury epicenter were dissected out 3 and 10 days and 4 and 8 weeks post-injury ($n = 3$/time point) and homogenized in ice-cold lysis buffer containing 1× protease inhibitor cocktail and phosphatase inhibitors. The protein concentration was determined using a BCA protein assay kit (Pierce). The extracted proteins were analyzed in a 10% polyacrylamide-SDS gel and electroblotted using a nitrocellulose membrane. After blocking, the membranes were probed overnight at 4 °C with rabbit anti-KIF2A polyclonal antiserum (1:1000; Abcam, Cambridge, MA, USA), anti-GAPDH (1:2000), anti-phospho-CDK5 (1:500) and anti-phospho-PAK1 (Thr 423) (1:500) (the last three from Santa Cruz Technologies, CA). Afterward, HRP-conjugated donkey anti-rabbit or anti-mouse IgG, respectively (1:10,000; Sigma, St. Louis, MO), were applied to the membrane and incubated for 1 h at room temperature. Blots were visualized using the ECL-plus kit (Amersham-Pharmacia Biotech). Densitometric analysis was performed using ImageJ™ software. The levels of KIF2A standardized to the amount of immunodetected GAPDH at each time point were studied.

Results

We examined the expression of KIF2A in primary cortical cultures by immunocytochemistry and found that it was expressed in the growth cones, cell body and to a weaker extent along the length of the neurites that we labeled with an antibody to beta-3 tubulin (Fig. 1a, b). Liposome-mediated delivery of KIF2A-siRNA to the cortical neurons significantly increased their axonal length and branching, but not the total number of branches (total number of "end points") (Supplementary Figure 2). The quantitative assessment of the neurite outgrowth showed a significant increase in length of the axonal and collateral branches of the cortical neurons transfected with the lipid nanoparticles containing KIF2A-siRNA compared to transfection of the scrambled-siRNA (negative-Ctrl) or to non-transfected neurons (Ctrl) (mean ± SEM; Ctrl-siRNA 102.6 ± 4.2 µm or negative-Ctrl-siRNA 81.16 ± 4.2 µm vs KIF2A-siRNA 119.58 ± 7.9 µm for axonal length; and Ctrl- siRNA 15.12 ± 0.48 µm or negative-Ctrl-siRNA 14.37 ± 0.57 µm vs KIF2A-siRNA 18.14 ± 0.94 µm for collateral branches length) (Fig. 1c–f). Unexpectedly, we observed a reduction in axonal length with the scrambled siRNA. A possible off-target effect of the scrambled siRNA seems to be the most plausible explanation for this effect. Indeed, commercial scrambled controls may have off-target effects depending on cellular contexts [65]. These data are consistent with previous observations by Homma et al. [30] and Noda et al. [53] using hippocampal neurons, and indicate that KIF2A plays an inhibitory role in neurite outgrowth in the mammalian CNS (Fig. 1).

We subsequently asked whether KIF2A is expressed in the normal and injured spinal cord using western blotting and normalization to GAPDH after the dorsolateral funiculus (DLF) crush. An increase in KIF2A protein levels was noticeable on day 3 post-injury and this expression reached a significant 1.8-fold elevation by 4 weeks post-injury (wpi) that was sustained and even higher for 8 weeks post-injury (Fig. 1g) ($^*p < 0.05$).

Immunohistochemistry of sagittal sections was used to localize the expression of KIF2A following SCI. We found an increase in KIF2A immunoreactivity (IR) in the vicinity of the injury site by 10 days post-injury (Fig. 2a–a′, b), consistent with the increased in KIF2A protein as detected by western blotting (Fig. 1g). However, this lesion edge is prone to non-specific immunoreactions. To investigate the cellular location of KIF2A, double-label immunohistochemistry combined with confocal analysis with antibodies to β-III-tubulin (axons), GFAP (astrocytes), PDGFRα (OPCs, oligodendrocyte progenitor cells and a subpopulation of vascular pericytes) and CC1 (mature oligodendrocytes) was performed (Fig. 2). There was high expression of KIF2A in a subpopulation of CC1$^+$ cells in the areas adjacent to the injury site. However, we did not find any increase in KIF2A expression in mature oligodendrocytes located near the injury when compared with the more distant areas from the epicenter (Fig. 2b, d). Moreover, at the time points analyzed, we did not detect co-expression of KIF2A in GFAP$^+$ or PDGFRα$^+$ cells in the vicinities of the injury (Fig. 2a–a′, c, f), suggesting that the protein was not expressed in astrocytes or OPCs following SCI. A weaker basal KIF2A expression was present in axons and neurons ~ 2 mm from the injury site (Fig. 2g), and that expression in axons gradually decreased as we looked further away from the injury site as seen in Fig. 7c. Similar levels of KIF2A expression were observed in cervical and thoracic areas from uninjured spinal cords (Supplementary Figure 3).

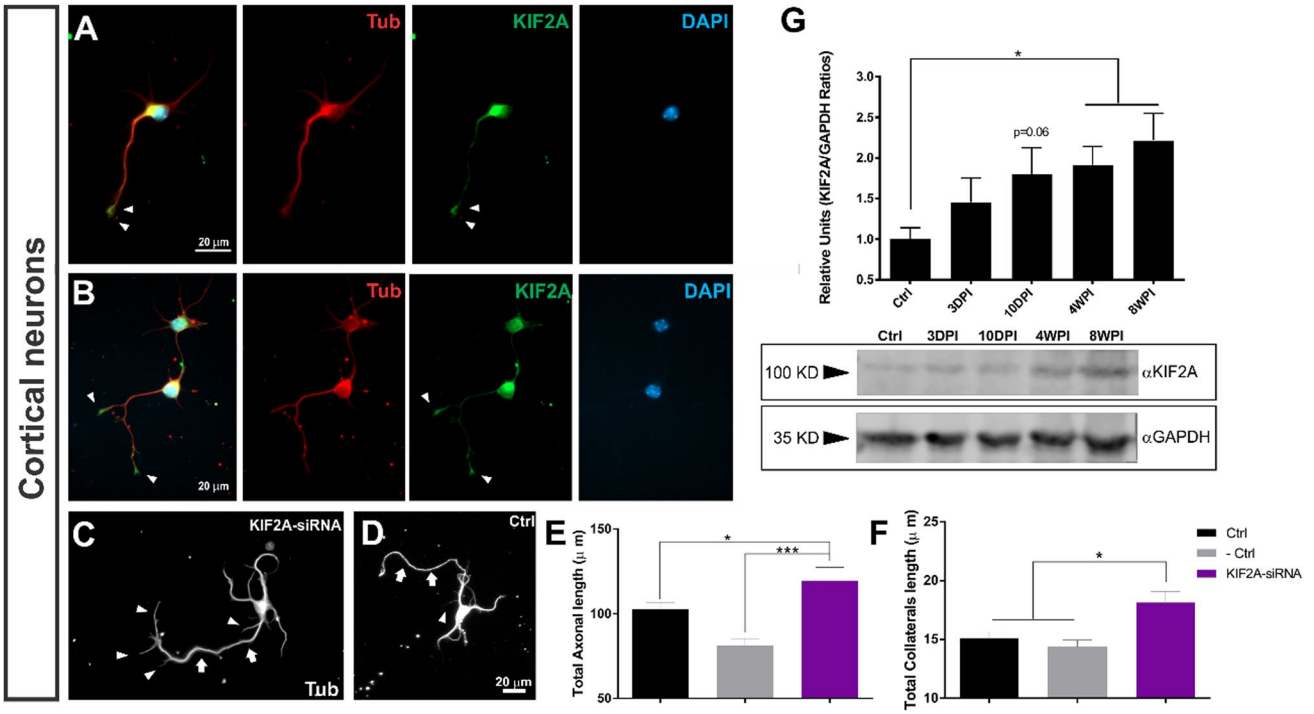

Fig. 1 Representative examples **a**, **b** of primary cortical neurons labeled with KIF2A antibody (green), tubulin (red) and DAPI. The arrowheads show the growth cones. **c**, **d** Representative images (tubulin) of a KIF2A knockdown and a control cortical neuron. Arrows show the axon and arrowheads point to the collateral branches. **e** Total axon length measurement (*$p<0.035$, ***$p<0.0001$) and total collateral branches length (*$p<0.035$) **f** for non-lipofected neurons; and scrambled-siRNA (negative control) and KIF2A-siRNA lipofected cortical neurons. The data are mean ± SEM. Control ($n=272$), negative control ($n=85$), KIF2A-siRNA ($n=95$); from three different experiments. **g** Western blot time-course analysis after SCI. The data are mean ± SEM ($n=3$, *$p<0.05$). All statistics are one-way ANOVA with Fisher's LSD test

Sections containing gray matter of the injured spinal cords revealed a pronounced expression of KIF2A in cells with neuron-like cell morphology with typical oval-shaped, triangular or irregular bipolar or multipolar appearance. Double immunohistochemistry for KIF2A in combination with the neuronal marker NeuN revealed co-expression of KIF2A with NeuN in the gray matter (Fig. 3).

Parvalbumin (Parv) and calbindin (Calb), markers for inhibitory interneurons, were used in an effort to better characterize the NeuN$^+$ neurons that were KIF2A positive. Interestingly, we found parvalbumin and calbindin co-expression with KIF2A$^+$ neurons both rostral and caudal to the injury site (Fig. 4a, b). As expected, we did not find neurons expressing high levels of KIF2A in the intact spinal cord at either the cervical or thoracic levels. Moreover, Parv$^+$ and Calb$^+$ neurons were distributed homogeneously in the uninjured spinal cord as well as in the vicinities of the lesion after SCI in the rostro-caudal axis (Supplementary Figure 3). KIF2A and parvalbumin were found to be co-expressed in some cells, whereby the levels of expression of parvalbumin varied (Fig. 4a′–a″).

Calbindin distribution among the KIF2A$^+$ cells was similar to what we observed for parvalbumin (Fig. 4b). Calbindin and parvalbumin immunoreactivity was localized throughout the neuronal cytoplasm and some Calb$^+$ neurons showed a punctate cytoplasmic expression as previously described (Fig. 4b′) [52]. In both immunostaining experiments, we detected single-labeled KIF2A$^+$, Parv$^+$ and Calb$^+$ cells distributed adjacent to the injury site (Fig. 4a, b). Additionally, to determine the percentage of KIF2A$^+$ cells expressing parvalbumin and calbindin, the total amount of cells that were either KIF2A$^+$, Parv$^+$ or Calb$^+$ was counted from three different fields from each spinal cord ($n=4$). As shown in

Fig. 2 Double immunofluorescent staining for KIF2A and different specific cellular markers 10 days after dorsolateral funiculus (DLF) crush. **a**, **b**, **g** Low-power views of sagittal sections immunostained for KIF2A together with antibodies for specific cellular markers such as β-III-tubulin (Tub, for neurons in **a** and **g**), CC1 (for oligodendrocytes in **b**) and GFAP (for astrocytes **a**, **b** and **g**) (**a′** are zoomed in magnification of the boxed area in **a**). **c**–**f** High-power micrographs taken at the vicinities of the injury site stained for KIF2A and for specific markers: PDGFRα (for oligodendrocyte progenitor cells and a subpopulation of vascular pericytes), CC1, β-III-tubulin and GFAP (for astrocytes). All high-power micrographs come from **b,** but the one in **c** was taken from a different section (not shown). Arrowheads show co-localization of KIF2A with β-III tubulin (**e**) and CC1 (**d**) but no co-localization of PDGFRα (**c**) or GFAP (**f**) with KIF2A

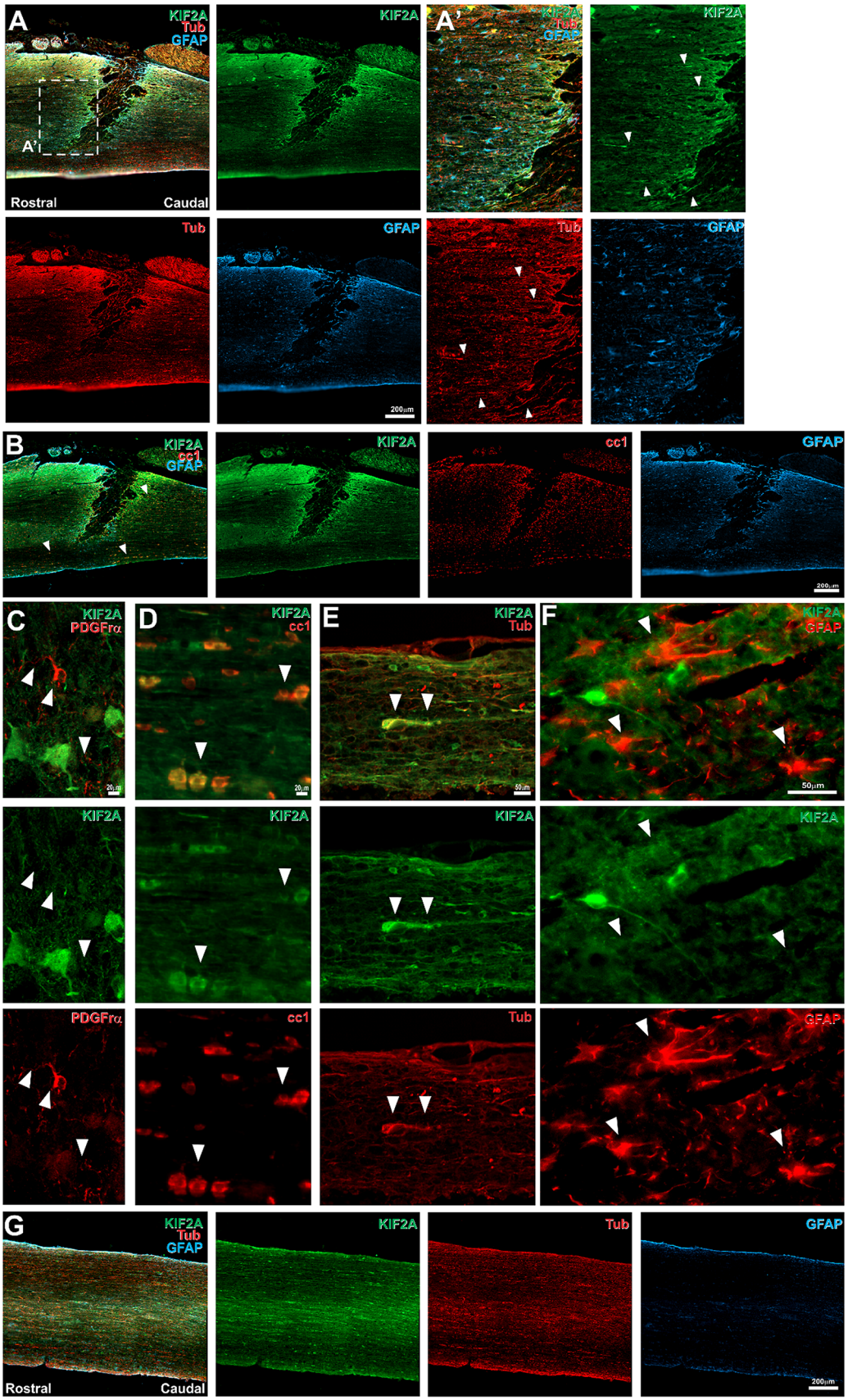
A
KIF2A
Tub
GFAP
A'
Rostral
Caudal
KIF2A
Tub
GFAP
200μm
B
KIF2A
cc1
GFAP
C
KIF2A
PDGFrα
20μm
D
KIF2A
cc1
E
KIF2A
Tub
50μm
F
KIF2A
GFAP
PDGFrα
G

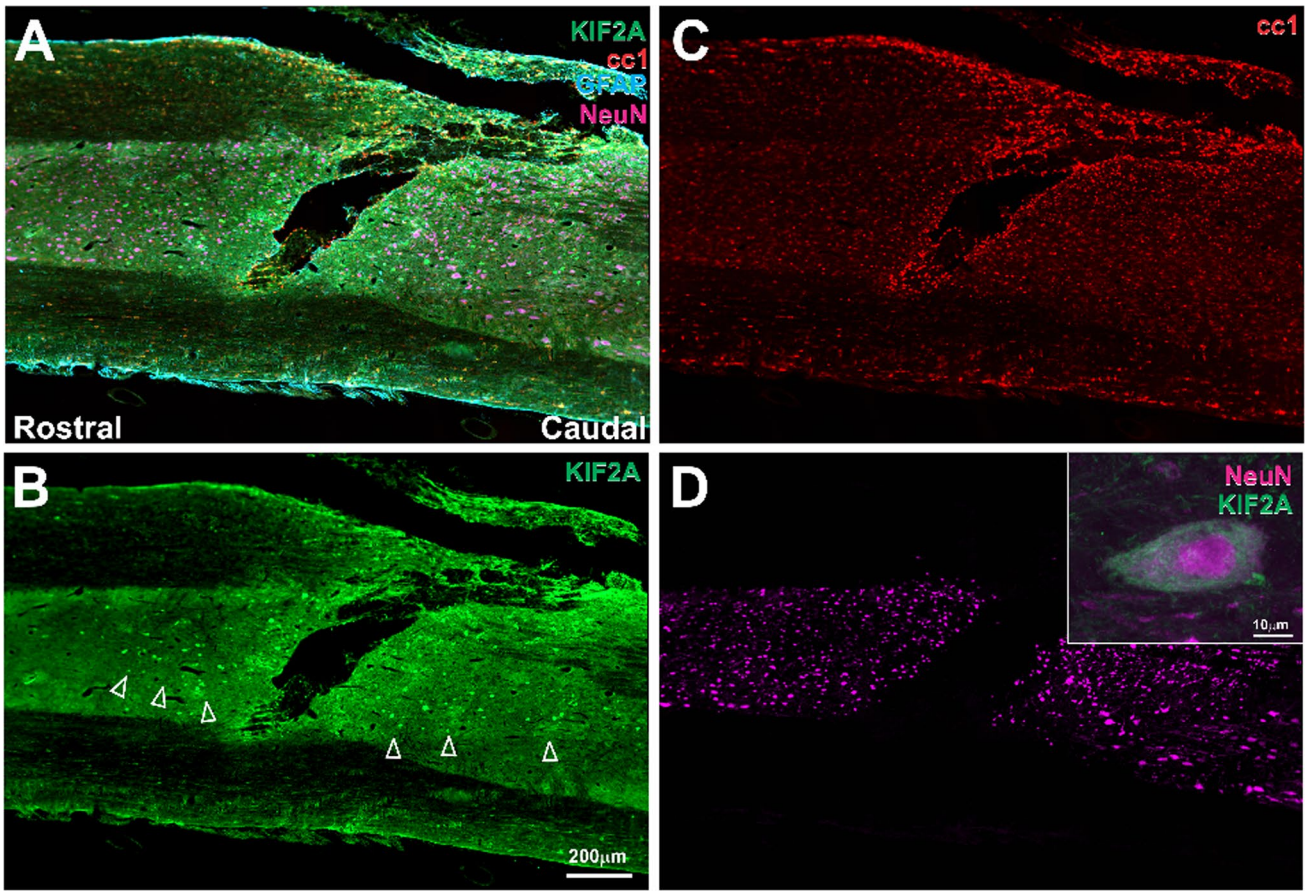

Fig. 3 Immunofluorescent stainings for KIF2A in sagittal sections from injured spinal cord 10 days after DLF crush. **a**–**d** KIF2A staining with CC1, GFAP and NeuN markers. Open arrowheads show a group of KIF2A$^+$ neurons. Boxed inset shows a KIF2A$^+$ neuron at higher magnification

Fig. 4, we found that 28% of cells co-expressed both KIF2A and parvalbumin. The proportion of cells expressing only KIF2A was 24%, and the ones expressing only parvalbumin 48% (Fig. 4c). On the other hand, 37% of cells co-expressed KIF2A and calbindin, and the proportion of cells expressing only KIF2A was 3%. The percentage of cells expressing only calbindin was 60% (Fig. 4d), therefore, suggesting that after SCI a significant number of inhibitory interneurons (28% Parv$^+$, 37% Calb$^+$) express high levels of KIF2A.

Transection/crush models are important to determine strategies designed to promote axonal sprouting and regeneration, but blunt models are widely used in rodents because of their morphological, histological, and functional similarities to human SCI [1, 9, 10, 46]. Thus, we performed two different spinal cord contusion injuries (C4–C5 and T8–T9) to complement our results observed in the DLF crush model.

High KIF2A immunoreactivity was found in the spared tissue and axons in the ipsilateral side of the cord (epicenter and up to ± 1 mm) compared to the contralateral side after cervical C5 hemicontusion 8 weeks post-injury (Fig. 5). To further investigate the cell location of KIF2A and in an effort to complement the characterization performed in the DLF crush model, double-label immunohistochemistry analysis with antibodies to NF200 (axons), Chat1 (motoneurons), PDGFRβ (pericytes) and CC1 (mature oligodendrocytes), Iba1 (microglia) and CD45 (macrophages) was performed (Fig. 5). KIF2A was highly expressed in spinal neurons in the ipsilateral gray matter, but not in motoneurons in the ventral horn (Fig. 5a–a′). In Fig. 5c, we quantified the number of high KIF2A$^+$ cells 2.5 mm rostral and caudal from the epicenter of the injury. KIF2A$^+$ cells were present in the vicinities of the injury, but their numbers decreased, both rostral and caudal, past 1.5 mm distance from the epicenter. Interestingly, we noticed a higher number of KIF2A$^+$ cells below the injury site when compared to the sections from above (Fig. 5c). The cell counts represent an underestimation of the real cell numbers as a result of the methodology used for the counting (see "Materials and methods").

KIF2A immunoreactivity was also elevated in a subpopulation of mature oligodendrocytes in our cervical hemicontusion cords, similarly to what we observed in our DLF crush model (Fig. 2d). However, we did not see any differences

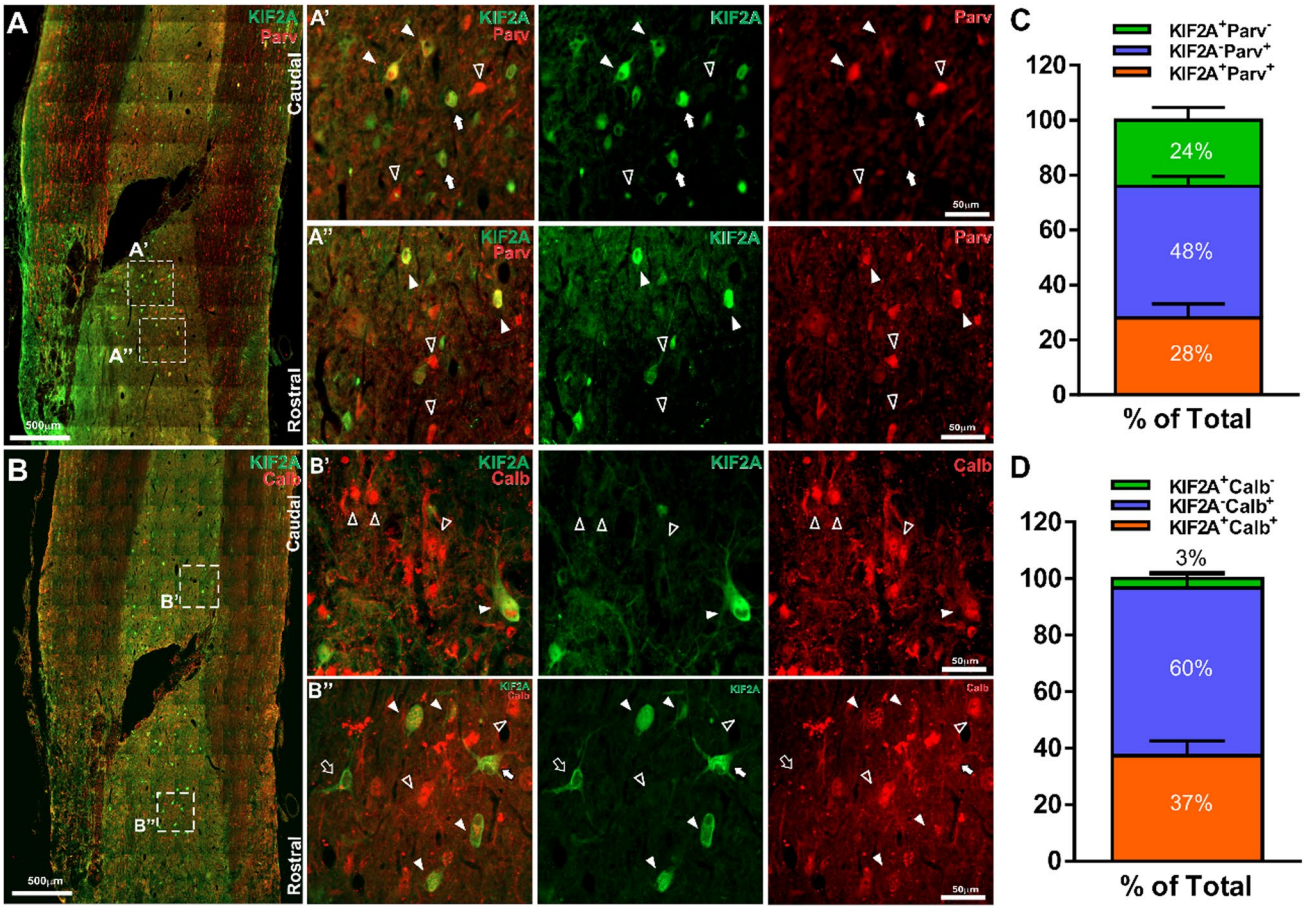

Fig. 4 Immunofluorescent stainings in sagittal sections from injured spinal cord (10 days after DLF crush) with interneuron calcium-binding protein markers. **a** Low-power magnification showing the immunostainings for KIF2A and parvalbumin. **a′**–**a″** High magnifications of the boxed areas. Solid arrowheads and open arrowheads show KIF2A$^+$/Parv$^+$ and KIF2A$^-$/Parv$^+$ cells, respectively. Arrows in **a″** show Parv$^+$ with lower levels of parvalbumin in cells with high KIFA content. **b** Low-power magnification showing the staining with antibodies to KIF2A and calbindin. **b′**–**b″** High magnifications of the boxed areas. Solid arrowheads and open arrowheads show KIF2A$^+$/Calb$^+$ and KIF2A$^-$/Calb$^+$ cells, respectively. The arrow shows an example of KIF2A$^+$/Calb$^+$ cell with lower calbindin expression and the open arrow shows one example of a KIF2A$^+$/Calb$^+$ cell. **c**, **d** Quantitative analysis of the two different populations of interneurons expressing KIF2A (percentage of total cells counted) in injured spinal cord. The data are mean ± SEM

in KIF2A expression in CC1$^+$ cells between the ipsilateral and contralateral side of the cord in the vicinities of the injury or far away from the epicenter (Fig. 5a″–a‴; Supplementary Figure 4). Furthermore, KIF2A did not co-localize with microglia, macrophage (Fig. 5b) or pericyte markers (Fig. 5d), suggesting that KIF2A is not expressed in these cell types 8 weeks post-SCI.

Our observations to this point seemed to suggest that the increase in expression of KIF2A was restricted to axons and spinal interneurons near the injury site after SCI. Hence, in an effort to better understand the nature of those axons, we co-stained horizontal sections using markers to target serotonergic (5-HT) and corticospinal (PKCγ) [18, 38, 49, 51, 58] axonal projections (Fig. 6a, b). KIF2A was highly expressed in injured axons at the vicinities of the injury site. Moreover, we found that some of those axons co-localized with serotonergic axons in the spared white matter (Fig. 6a, a′, b′), but also on what it seems like sprouted axons located in areas of the gray matter closer to the injury site (Fig. 6a, c′, d′). 5-HT$^-$ KIF2A$^+$ axons were also found in the vicinities of the injury (Fig. 6e′). Similarly to the serotonergic axons, we also observed co-localization between axons expressing elevated contents of KIF2A and PKCγ in the spared white matter (Fig. 6b, f′, g′). These results suggest that KIF2A increases in diverse types of axonal projections after SCI, including serotonergic axons, which has been previously associated with spasticity and pain following spinal cord injury [50], and corticospinal axons, associated with locomotor control [4].

Furthermore, when we examined the spinal cords from animals that underwent a T9 midline contusion, KIF2A was also present in axons in the white matter (Fig. 7a–a″) and

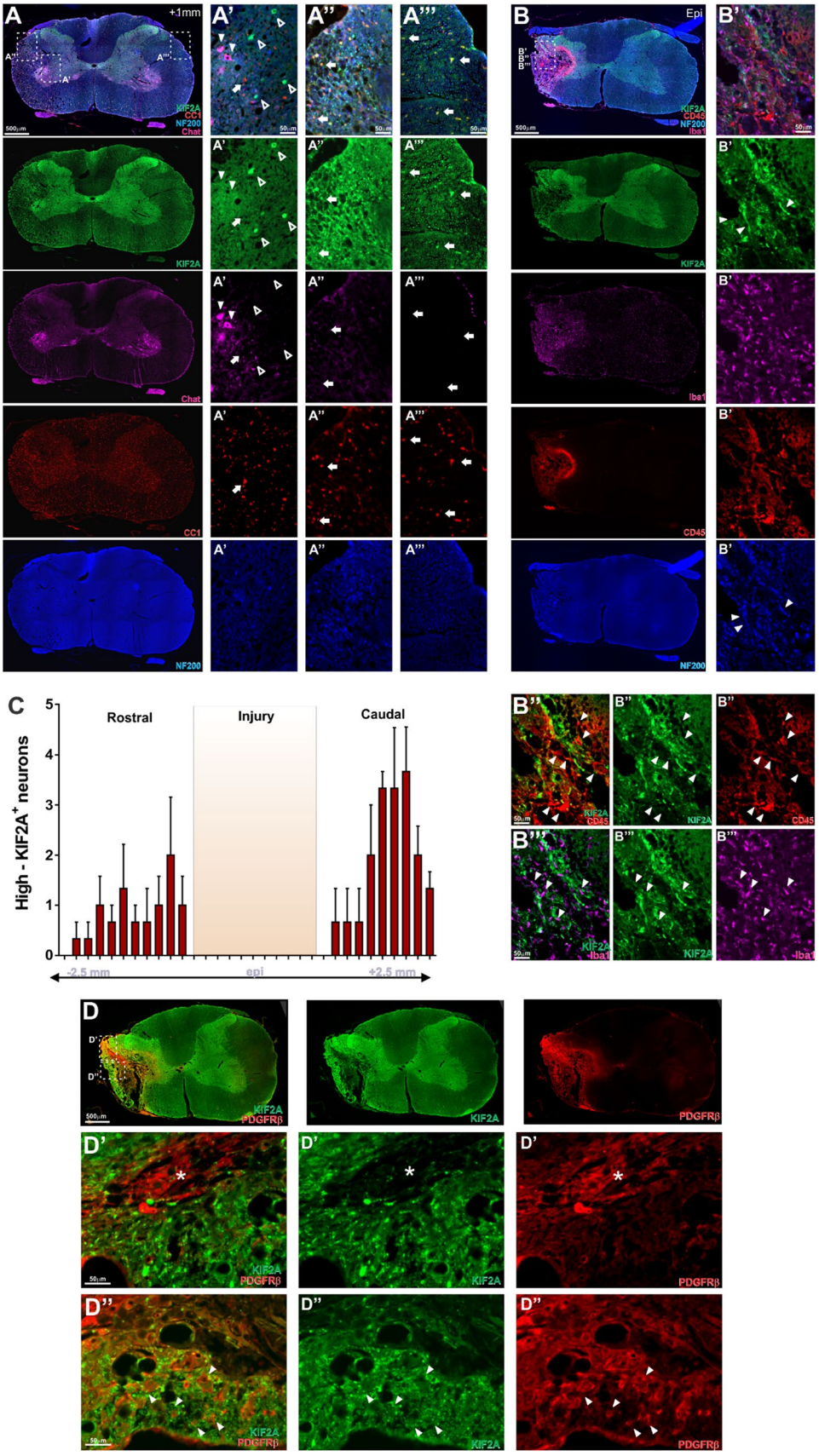
A
+1mm
A'
A''
A'''
KIF2A
CC1
NF200
Chat
B
Epi
B'
B''
KIF2A
CD45
NF200
Iba1
Chat
CC1
CD45
NF200
C
High - KIF2A+ neurons
Rostral
Injury
Caudal
-2.5 mm
epi
+2.5 mm
B''
B'''
KIF2A
CD45
Iba1
D
D'
D''
KIF2A
PDGFRβ
*

◂**Fig. 5** Double immunofluorescent staining for KIF2A and different specific cellular markers 8 weeks after C5 cervical hemicontusion. Low-power views of cross sections from caudal (**a**) or epicenter (**b**, **d**) regions immunostained for KIF2A together with antibodies for specific cellular markers such as NF200 (for neurofilaments), CC1 (for oligodendrocytes in **a**), Chat1 (for motoneurons in **a**), Iba1 (for microglia in **b**), CD45 (for macrophages in **b**) and PDGFRβ (for pericytes in **d**). **a′**, **a″**, **a‴** Zoomed-in magnifications of the boxed areas in **a**. **a′** High-power micrograph of the ventromedial gray matter of the ipsilateral (injured) side of the cord. Arrowheads show Chat1$^+$ motoneurons, open arrowhead shows cells with high KIF2A content and arrow shows an example of a CC1$^+$ cell with very low KIF2A content. **a″**–**a⁗** High-power micrographs of the ipsilateral (**a″**) and contralateral (**a⁗**) white matter. Arrows indicate CC1$^+$ with high KIF2A content in both areas. Notice the increased KIF2A expression in the ipsilateral side (**a″**) that corresponds to the increased levels of KIF2A in the axons in the vicinities of the injury. **b′**, **b″**, **b‴** Zoomed in magnifications of the boxed area in **b**. **b′** Quadruple co-staining images. Arrowheads indicate axons with high immunoreactivity for KIF2A at the epicenter of the injury. **b″**, **b‴** show double co-staining between KIF2A and CD45 or Iba1 in the epicenter of the injury. Notice no co-localization of KIF2A with these specific cell markers (arrowheads). **c** Quantifications of the number of high KIF2A$^+$ expressing neurons in the gray matter along the spinal cord. Note the increased number of KIF2A$^+$ neurons in the vicinities of the injury, and the peak in KIF2A$^+$ neurons around 1 mm from the injury site in the caudal region. The data are mean ± SEM. All sections up to + 2.5 mm rostral and − 2.5 mm caudal from the epicenter were counted from three different animals. **d′**, **d″** Zoomed in magnifications of the boxed area in **b** showing no co-localization of KIF2A and PDGFRβ in two different areas of the epicenter of the injury. Asterisk shows an accumulation of pericytes in the injury site. Arrowheads show examples of infiltrated KIF2A$^-$ pericytes in the spared white matter

expressed by CC1$^+$ cells and its processes in both gray and white matter (Fig. 7b, b′). KIF2A staining was increased at the tips of injured axons as well as in axons in the spared rim adjacent to the injury site (Fig. 7c, d). A noteworthy subpopulation of the mature oligodendrocytes expressed high KIF2A contents (Fig. 7e, e′). Similarly to what we observed in the DLF crush and the cervical C5 hemicontusion models, KIF2A immunoreactivity was remarkably enhanced in a group of NeuN$^+$ neurons adjacent to the lesion site (rostral and caudally) (Fig. 7e).

Altogether, our results reveal that KIF2A is expressed in neuronal structures and oligodendrocytes after three different mechanisms of SCI, and that its expression is sustained for an extended period after injury.

Discussion

We show here for the first time the pattern of expression of kinesin KIF2A, localization and distribution after SCI. While the expression of KIF2A in the uninjured spinal cord was low, our findings indicate that after traumatic SCI KIF2A is expressed at the right time and place to play a role in the inhibition of axonal branching and regeneration. The highly localized expression of KIF2A in a subpopulation of interneurons in the gray matter, and in serotonergic and corticospinal projections, suggests a possible role in the control of central neuropathic pain and/or even possibly in locomotor control and spasticity.

Possible involvement of KIF2A and other kinesins in repair

Our results demonstrate an upregulation of KIF2A protein levels following rat SCI which reached a plateau at 10 dpi and were sustained until 8 wpi. Confocal analysis of KIF2A distribution revealed its presence in neuronal cell bodies and injured axon tips adjacent to the epicenter of the lesion. In this regard, other studies demonstrate that members of the kinesin family are involved in controlling regeneration. For example, kinesin-5 inhibition with monastrol promotes neurite outgrowth of DRG neurons on inhibitory substrates in vitro [3, 39] and regeneration after complete thoracic spinal cord transection when combined with ChABC [71]. However, when KIF3C, an MT-destabilizing factor member of the kinesin-2 family, is lost, there is an impairment in axonal outgrowth in both embryonic and adult DRG neurons in vitro and in vivo [26]. KIF3C is also implicated in microglial and astrocytic proliferation in the adult rat spinal cord following injury [73]. Kinesin-13 is downregulated after injury in *C. elegans,* altering cytoskeletal MT dynamics and enhancing regrowth [23]. KIF2A is only expressed in mature oligodendrocytes but not in OPCs or astrocytes in the spinal cord, contrary to what is observed for KIF3B 5 days after a contusion injury at the thoracic level (T9) [73].

Interestingly, some kinesin motor family proteins (i.e., KIF14, KIF1B) play a role in myelination through the control of cargo transportation along oligodendrocyte processes [22, 42]. However, in our models we did not observe an increase in KIF2A expression in mature oligodendrocytes in the areas adjacent to the epicenter compared to other areas distant from the injury site (Supplementary Figure 4). We observed basal high levels of KIF2A in a subpopulation of oligodendrocytes (Supplementary Figure 4). In fact, those differences in basal expression levels among the mature oligodendrocyte population might be associated with the heterogeneity in the oligodendroglial subpopulations in the CNS [36, 44, 69]. Since it is already well established that there is an increase in the mature oligodendrocyte population after injury over time [63, 75], we can not fully discard that it might, in part, be contributing to the increased expression of KIF2A in in the injury site. Overall, this suggests that in mature oligodendrocytes, KIF2A might function only as a motor protein and would not have a role in oligodendrocyte plasticity as we see in neurons.

Previous work from Ogawa demonstrates that KIF2A undergoes site-specific phosphorylation, differentially affecting neuronal morphogenesis during development [55]. Thus,

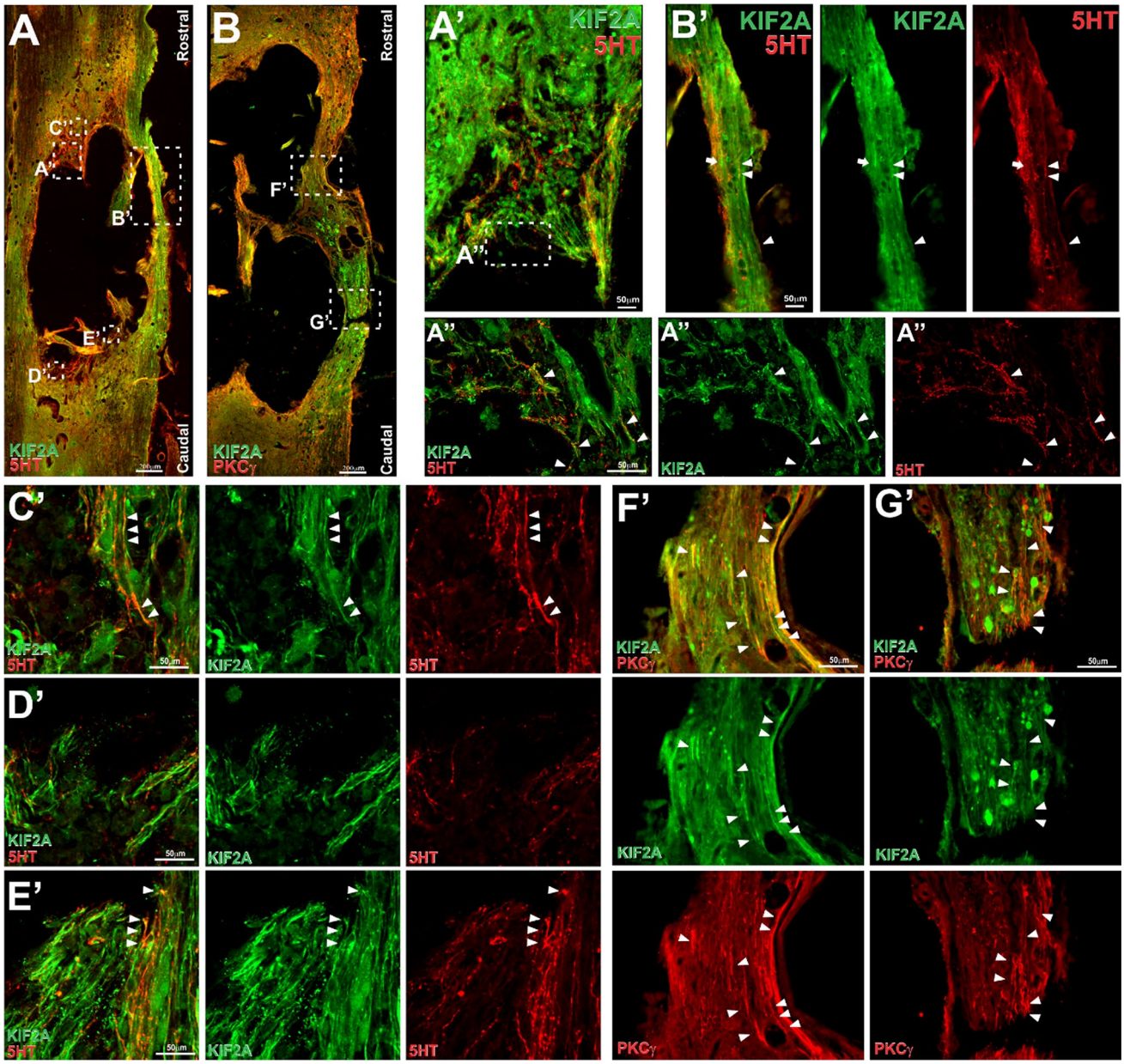

Fig. 6 Double immunofluorescent staining for KIF2A and 5-HT (serotonin transporter) or PKCγ [gamma isotype of protein kinase C, found in corticospinal tract axons (CST)] 8 weeks after C5 cervical hemicontusion. **a**, **b** Low-power views of horizontal sections at the epicenter of the injury. Asterisks shows the cavity. **a′**–**g′** High-power magnifications of the boxed areas in **a**, **b**. **a′**–**d′** Different examples of areas were highly immunoreactive axons for KIF2A are 5-HT^{+} (arrowheads) or 5-HT^{-} (arrows). An example of an area with no 5-HT^{+} axons is shown in **e′**. **f′**, **g′** High-power micrographs showing examples of co-localization (arrowheads) between highly KIF2A immunoreactive axons and PKCγ in the vicinities of the injury

an increase in phosphorylation in its A-type site promotes inhibition of the depolymerization activity and neurite growth arrest (via ROCK), while an increase in its B-type site (via PAK1 and CDK5 activation) induces an increase in MT depolymerization and consequently neurite outgrowth. Based on Ogawa's study, it could seem that the increase in KIF2A in axons and neurons after SCI could be an attempt of the neurons to growth rather than to prevent axonal or collateral branches growth. However, our data suggest that changes in CDK5 and PAK1 activity occur in the acute, but not in the chronic phase after injury (Supplementary Figure 5). Interestingly, Noda's and colleagues work shows that in in vitro assays, phosphatidylinositol 4-phosphate 5-kinase (PIPKα) enhances MT depolymerization and suppresses axonal branches elongation via KIF2A [53]. Indeed, we know that PIPKα (PIP5K) is downstream of ROCK [7,

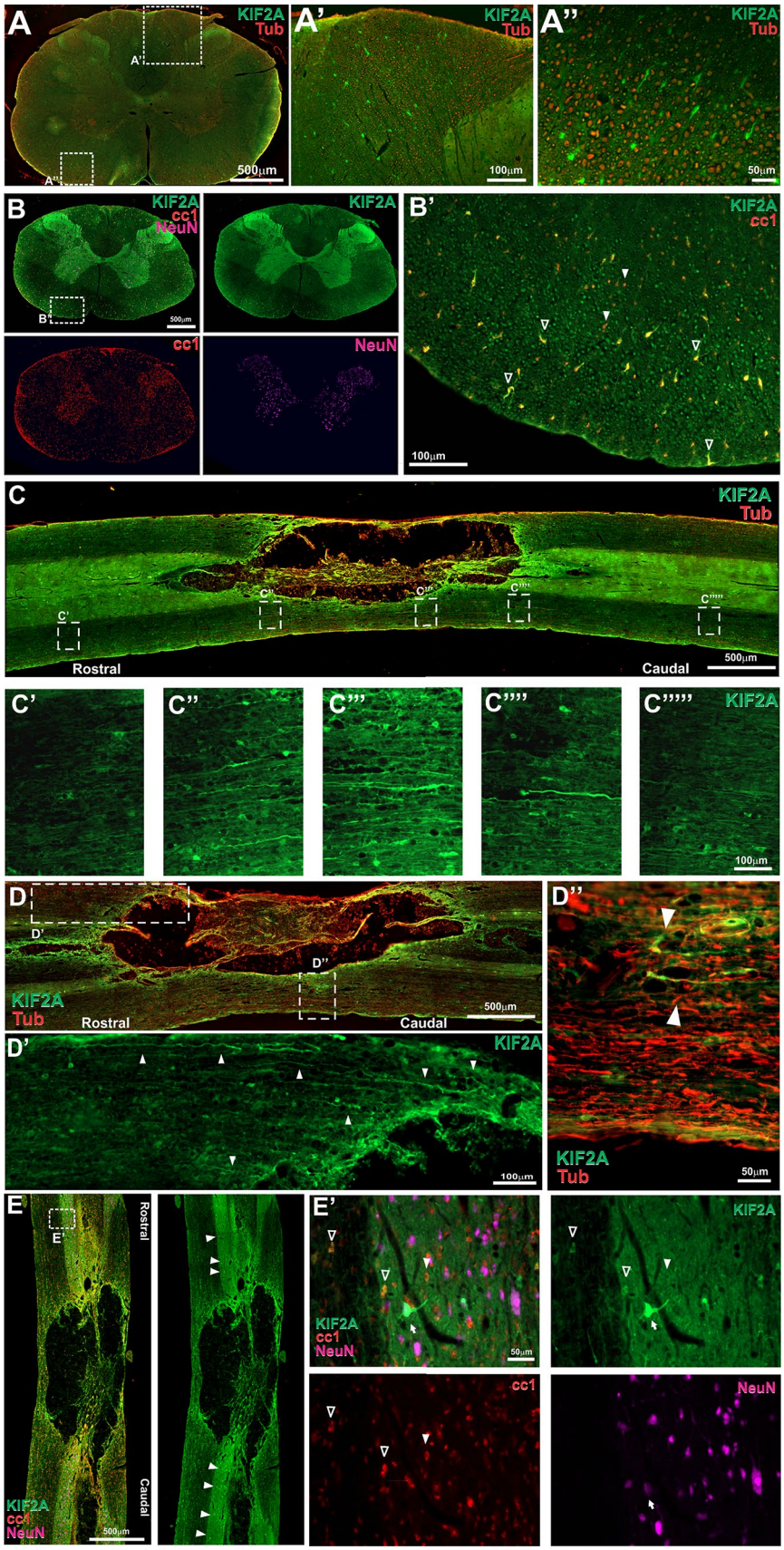

Fig. 7 Immunofluorescent staining for KIF2A and different cell specific markers 8 weeks after spinal cord contusion. **a**, **b** Low-power views of cross sections (5 mm rostral to epicenter) immunostained for KIF2A, beta-III-tubulin, CC1 and NeuN (**a′**, **a″**, **b′**, high magnification micrographs of the boxed areas in **a** and **b**, respectively. **c**, **d** Examples of sagittal sections immunostained for KIF2A and beta-III-tubulin. **c′**–**c′′′′**, **d′**, **d″** High magnifications of the boxed areas. Arrowheads show KIF2A$^+$ axons. **e** Horizontal section of the epicenter immunostained for KIF2A, CC1 and NeuN (arrowheads show KIF2A$^+$ cells). High magnification micrograph of the boxed area (**e′**). Arrow shows a NeuN$^+$ cell with high KIF2A content, open arrowheads show CC1$^+$/KIF2A$^+$ cells and the solid arrowhead shows a CC1$^+$ cell expressing weak levels of KIF2A

41, 72] and negatively regulates neurite outgrowth. It is also very well accepted in the field that the Rho–ROCK pathway has a master role in inhibition of axonal outgrowth after injury or after exposure to inhibitory substrates [5, 20]. So, it seems likely that the over-activation of this pathway might trigger an increase in KIF2A phosphorylation in its A-type over the B-type site, which in turn might induce MT depolymerization and inhibition of axonal and collateral branching growth after SCI.

Thus, KIF2A might mainly act as a neuronal injury-associated kinesin that contributes to axonal growth and branching inhibitory mechanisms by regulating and organizing the MT cytoskeleton in the axon and growth cone in acute and possibly chronic stages after SCI.

Possible role of KIF2A in central neuropathic pain (CNP) and spasticity

Central neuropathic pain (CNP) occurs following insults to the CNS such as SCI, stroke and multiple sclerosis [12]. CNP is caused by central disinhibition and/or central sensitization, but the exact mechanisms of pain are poorly understood. Disinhibition and sensitization lead to neuronal hyperactivity of spinal nociceptive neurons [2, 8, 17]. Numerous proteins play an important role in modulation of nociceptive signaling at the spinal cord level. Parvalbumin and calbindin calcium-binding proteins (CBP) are expressed by several inhibitory interneuronal populations in the spinal cord [37, 56, 59, 60]. Both are extensively used as markers of specific neuronal subsets. CBPs act as intracellular calcium buffers, and they have been suggested to modulate synaptic transmission at the spinal cord level [56, 74]. Consequently, a pathological increase in sensitivity (allodynia or hyperalgesia) after SCI is associated with changes in the modulation of these interneuron populations [15, 56].

Here, we observed that KIF2A was highly expressed in a distinct group of neurons in the gray matter, which are located adjacent to the injury epicenter in our DLF crush model. CBP^+ subpopulations of interneurons can be found commonly distributed in the different laminae in the gray matter. Thus, $Calb^+$ neurons are present in all laminae (I–X), while $Parv^+$ neurons are mostly distributed in laminae II–X, both with variable densities and numbers between laminae [9, 10, 61], suggesting that the group of $KIF2A^+$ neurons belongs to these populations. In fact, our immunoreactivity analyses demonstrated that 28% and 37% of $KIF2A^+$ neurons were positive for either parvalbumin or calbindin markers, respectively. We also found some degree of variability in the levels of expression of these markers possibly attributed to a downregulation in their expression after SCI as previously shown for spinal cord parvalbumin interneurons after peripheral nerve transection [56]. Moreover, since the DLF crush may sever a most medial part of the gray matter, we cannot exclude the possibility that some of the only $KIF2A^+$ neurons we observe in the vicinities of the injury, belong to different inhibitory interneurons with roles in locomotor control and/or spasticity. The Renshaw cells, for example, a subpopulation of interneurons located in the medial area of the gray matter, are $Calb^+$ and play a role in recurrent inhibition preventing hyperactivity of the motoneurons which consequently results in the control of muscle spasticity [16, 57].

Furthermore, our quantifications of the number of $KIF2A^+$ cells in the contused cords showed a higher number of KIF2A-positive cells below the injury level. In that regard, it is well established that after SCI, the intraspinal circuitry below the injury experiences a considerable remodeling that contributes to pain, spasms and other neurological dysfunctions after SCI (Fouad et al. [19]). It has also been previously shown that serotonergic axons are associated with spasticity and pain following spinal cord injury [50]. Our results show that some of the serotonergic projections express high levels of KIF2A near the injury site, which again might support a possible link between KIF2A and neuropathic pain.

Altogether, this first characterization suggests that KIF2A may regulate the cytoskeleton dynamics in some of those subpopulations of interneurons after injury. Whether this could lead to a maladaptive response, CNP or changes in locomotor control and spasticity remains to be shown.

Conclusions

In conclusion, we have characterized the expression of KIF2A in injured axons after SCI, and we have identified a subset of inhibitory interneurons ($Parv^+$ or $Calb^+$) that have previously been implicated in neuropathic pain as being $KIF2A^+$. This study opens up new possibilities for the assessment of potential therapeutic strategies for the treatment of neuropathic pain, spasticity and for the promotion of axonal regeneration.

Acknowledgements We thank all laboratory members for their help and suggestions, and especially we thank Dr. W. Plunet and Dr. B. Hilton for their valuable feedback on and input into the manuscript and review. Funding was provided by a Seed Grant from the Rick Hansen Foundation to the Blusson Integrated Cure Partnership. W. T. holds the John and Penny Ryan British Columbia leadership chair in spinal cord research.

References

1. Anderson TE, Stokes BT (1992) Experimental models for spinal cord injury research: physical and physiological considerations. J Neurotrauma 9(Suppl 1):S135–S142
2. Attal N, Bouhassira D (2004) Can pain be more or less neuropathic? Pain 110(3):510–511

3. Baas PW, Matamoros AJ (2015) Inhibition of kinesin-5 improves regeneration of injured axons by a novel microtubule-based mechanism. Neural Regen Res 10(6):845–849
4. Barbeau H, Fung J et al (2002) A review of the adaptability and recovery of locomotion after spinal cord injury. Prog Brain Res 137:9–25
5. Borisoff JF, Chan CC et al (2003) Suppression of Rho-kinase activity promotes axonal growth on inhibitory CNS substrates. Mol Cell Neurosci 22(3):405–416
6. Bradke F, Fawcett JW et al (2012) Assembly of a new growth cone after axotomy: the precursor to axon regeneration. Nat Rev Neurosci 13(3):183–193
7. Broggini T, Schnell L et al (2016) Plasticity Related Gene 3 (PRG3) overcomes myelin-associated growth inhibition and promotes functional recovery after spinal cord injury. Aging (Albany NY) 8(10):2463–2487
8. Casey KL (1992) 1991 Bonica Lecture. Central pain syndromes: current views on pathophysiology, diagnosis, and treatment. Reg Anesth 17(2):59–68
9. Chen K, Liu J et al (2016) Differential histopathological and behavioral outcomes eight weeks after rat spinal cord injury by contusion, dislocation, and distraction mechanisms. J Neurotrauma 33(18):1667–1684
10. Chen S, Yang G et al (2016) A comparative study of three interneuron types in the rat spinal cord. PLoS One 11(9):e0162969
11. Correas I, Diaz-Nido J et al (1992) Microtubule-associated protein tau is phosphorylated by protein kinase C on its tubulin binding domain. J Biol Chem 267(22):15721–15728
12. Costigan M, Scholz J et al (2009) Neuropathic pain: a maladaptive response of the nervous system to damage. Annu Rev Neurosci 32:1–32
13. Dent EW, Gertler FB (2003) Cytoskeletal dynamics and transport in growth cone motility and axon guidance. Neuron 40(2):209–227
14. Drewes G, Trinczek B et al (1995) Microtubule-associated protein/microtubule affinity-regulating kinase (p110mark). A novel protein kinase that regulates tau-microtubule interactions and dynamic instability by phosphorylation at the Alzheimer-specific site serine 262. J Biol Chem 270(13):7679–7688
15. Dubner R (1991) Pain and hyperalgesia following tissue injury: new mechanisms and new treatments. Pain 44(3):213–214
16. Fallah Z, Clowry GJ (1999) The effect of a peripheral nerve lesion on calbindin D28k immunoreactivity in the cervical ventral horn of developing and adult rats. Exp Neurol 156(1):111–120
17. Finnerup NB, Jensen TS (2004) Spinal cord injury pain—mechanisms and treatment. Eur J Neurol 11(2):73–82
18. Forgione N, Chamankhah M et al (2017) A mouse model of bilateral cervical contusion-compression spinal cord injury. J Neurotrauma 34(6):1227–1239
19. Fouad K, Torres-Espín A, Fenrich KK (2019) Mechanisms of behavioral changes after spinal cord injury. Disord Nerv Syst Mot Syst https://doi.org/10.1093/acrefore/9780190264086.013.245
20. Fournier AE, Takizawa BT et al (2003) Rho kinase inhibition enhances axonal regeneration in the injured CNS. J Neurosci 23(4):1416–1423
21. Franker MA, Hoogenraad CC (2013) Microtubule-based transport—basic mechanisms, traffic rules and role in neurological pathogenesis. J Cell Sci 126(Pt 11):2319–2329
22. Fujikura K, Setsu T et al (2013) Kif14 mutation causes severe brain malformation and hypomyelination. PLoS One 8(1):e53490
23. Ghosh-Roy A, Goncharov A et al (2012) Kinesin-13 and tubulin posttranslational modifications regulate microtubule growth in axon regeneration. Dev Cell 23(4):716–728
24. Goold RG, Gordon-Weeks PR (2004) Glycogen synthase kinase 3beta and the regulation of axon growth. Biochem Soc Trans 32(Pt 5):809–811
25. Gordon-Weeks PR, Fournier AE (2014) Neuronal cytoskeleton in synaptic plasticity and regeneration. J Neurochem 129(2):206–212
26. Gumy LF, Chew DJ et al (2013) The kinesin-2 family member KIF3C regulates microtubule dynamics and is required for axon growth and regeneration. J Neurosci 33(28):11329–11345
27. Hirokawa N, Noda Y et al (2009) Kinesin superfamily motor proteins and intracellular transport. Nat Rev Mol Cell Biol 10(10):682–696
28. Hirokawa N, Takemura R (2005) Molecular motors and mechanisms of directional transport in neurons. Nat Rev Neurosci 6(3):201–214
29. Hirokawa N, Tanaka Y (2015) Kinesin superfamily proteins (KIFs): various functions and their relevance for important phenomena in life and diseases. Exp Cell Res 334(1):16–25
30. Homma N, Takei Y et al (2003) Kinesin superfamily protein 2A (KIF2A) functions in suppression of collateral branch extension. Cell 114(2):229–239
31. Homma N, Zhou R et al (2018) KIF2A regulates the development of dentate granule cells and postnatal hippocampal wiring. Elife. https://doi.org/10.7554/eLife.30935
32. Hur EM, Saijilafu et al (2012) Growing the growth cone: remodeling the cytoskeleton to promote axon regeneration. Trends Neurosci 35(3):164–174
33. Kapitein LC, Hoogenraad CC (2015) Building the neuronal microtubule cytoskeleton. Neuron 87(3):492–506
34. Kevenaar JT, Hoogenraad CC (2015) The axonal cytoskeleton: from organization to function. Front Mol Neurosci 8:44
35. Kim YT, Hur EM et al (2011) Role of GSK3 signaling in neuronal morphogenesis. Front Mol Neurosci 4:48
36. Kitada M, Rowitch DH (2006) Transcription factor co-expression patterns indicate heterogeneity of oligodendroglial subpopulations in adult spinal cord. Glia 54(1):35–46
37. Labrakakis C, Lorenzo LE et al (2009) Inhibitory coupling between inhibitory interneurons in the spinal cord dorsal horn. Mol Pain 5:24
38. Lieu A, Tenorio G et al (2013) Protein kinase C gamma (PKCgamma) as a novel marker to assess the functional status of the corticospinal tract in experimental autoimmune encephalomyelitis (EAE). J Neuroimmunol 256(1–2):43–48
39. Lin S, Liu M et al (2011) Inhibition of kinesin-5, a microtubule-based motor protein, as a strategy for enhancing regeneration of adult axons. Traffic 12(3):269–286
40. Liu G, Dwyer T (2014) Microtubule dynamics in axon guidance. Neurosci Bull 30(4):569–583
41. Liu T, Lee SY (2013) Phosphatidylinositol 4-phosphate 5-kinase alpha negatively regulates nerve growth factor-induced neurite outgrowth in PC12 cells. Exp Mol Med 45:e16
42. Lyons DA, Naylor SG et al (2009) Kif1b is essential for mRNA localization in oligodendrocytes and development of myelinated axons. Nat Genet 41(7):854–858
43. Maor-Nof M, Homma N et al (2013) Axonal pruning is actively regulated by the microtubule-destabilizing protein kinesin superfamily protein 2A. Cell Rep 3(4):971–977
44. Marques S, Zeisel A et al (2016) Oligodendrocyte heterogeneity in the mouse juvenile and adult central nervous system. Science 352(6291):1326–1329
45. Meijering E, Jacob M et al (2004) Design and validation of a tool for neurite tracing and analysis in fluorescence microscopy images. Cytom A 58(2):167–176

46. Metz GA, Curt A et al (2000) Validation of the weight-drop contusion model in rats: a comparative study of human spinal cord injury. J Neurotrauma 17(1):1–17
47. Monteiro MI, Ahlawat S et al (2012) The kinesin-3 family motor KLP-4 regulates anterograde trafficking of GLR-1 glutamate receptors in the ventral nerve cord of *Caenorhabditis elegans*. Mol Biol Cell 23(18):3647–3662
48. Morfini G, Quiroga S et al (1997) Suppression of KIF2 in PC12 cells alters the distribution of a growth cone nonsynaptic membrane receptor and inhibits neurite extension. J Cell Biol 138(3):657–669
49. Mori M, Kose A et al (1990) Immunocytochemical localization of protein kinase C subspecies in the rat spinal cord: light and electron microscopic study. J Comp Neurol 299(2):167–177
50. Nardone R, Holler Y et al (2015) Serotonergic transmission after spinal cord injury. J Neural Transm (Vienna) 122(2):279–295
51. Neumann S, Braz JM et al (2008) Innocuous, not noxious, input activates PKCgamma interneurons of the spinal dorsal horn via myelinated afferent fibers. J Neurosci 28(32):7936–7944
52. Ni Y, Nawabi H et al (2014) Characterization of long descending premotor propriospinal neurons in the spinal cord. J Neurosci 34(28):9404–9417
53. Noda Y, Niwa S et al (2012) Phosphatidylinositol 4-phosphate 5-kinase alpha (PIPKalpha) regulates neuronal microtubule depolymerase kinesin, KIF2A and suppresses elongation of axon branches. Proc Natl Acad Sci USA 109(5):1725–1730
54. Noda Y, Sato-Yoshitake R et al (1995) KIF2 is a new microtubule-based anterograde motor that transports membranous organelles distinct from those carried by kinesin heavy chain or KIF3A/B. J Cell Biol 129(1):157–167
55. Ogawa T, Hirokawa N (2015) Microtubule destabilizer KIF2A undergoes distinct site-specific phosphorylation cascades that differentially affect neuronal morphogenesis. Cell Rep 12(11):1774–1788
56. Petitjean H, Pawlowski SA et al (2015) Dorsal horn parvalbumin neurons are gate-keepers of touch-evoked pain after nerve injury. Cell Rep 13(6):1246–1257
57. Pierrot-Deseilligny E, Bussel B (1975) Evidence for recurrent inhibition by motoneurons in human subjects. Brain Res 88(1):105–108
58. Polgar E, Fowler JH et al (1999) The types of neuron which contain protein kinase C gamma in rat spinal cord. Brain Res 833(1):71–80
59. Porseva VV, Shilkin VV et al (2014) Calbindin-containing neurons of the ventral horn of murine spinal cord gray matter. Morfologiia 146(4):21–25
60. Porseva VV, Shilkin VV et al (2014) Subpopulation of calbindin-immunoreactive interneurons in the dorsal horn of the mice spinal cord. Tsitologiia 56(8):612–618
61. Ren K, Ruda MA (1994) A comparative study of the calcium-binding proteins calbindin-D28K, calretinin, calmodulin and parvalbumin in the rat spinal cord. Brain Res Brain Res Rev 19(2):163–179
62. Rishal I, Fainzilber M (2014) Axon-soma communication in neuronal injury. Nat Rev Neurosci 15(1):32–42
63. Rosenberg LJ, Zai LJ et al (2005) Chronic alterations in the cellular composition of spinal cord white matter following contusion injury. Glia 49(1):107–120
64. Sakakibara A, Ando R et al (2013) Microtubule dynamics in neuronal morphogenesis. Open Biol 3(7):130061
65. Scacheri PC, Rozenblatt-Rosen O et al (2004) Short interfering RNAs can induce unexpected and divergent changes in the levels of untargeted proteins in mammalian cells. Proc Natl Acad Sci USA 101(7):1892–1897
66. Seira O, del Rio JA (2014) Glycogen synthase kinase 3 beta (GSK3 beta) at the tip of neuronal development and regeneration. Mol Neurobiol 49(2):931–944
67. Sparling JS, Bretzner F et al (2015) Schwann cells generated from neonatal skin-derived precursors or neonatal peripheral nerve improve functional recovery after acute transplantation into the partially injured cervical spinal cord of the rat. J Neurosci 35(17):6714–6730
68. Vale RD (2003) The molecular motor toolbox for intracellular transport. Cell 112(4):467–480
69. van Bruggen D, Agirre E et al (2017) Single-cell transcriptomic analysis of oligodendrocyte lineage cells. Curr Opin Neurobiol 47:168–175
70. van den Berg R, Hoogenraad CC (2012) Molecular motors in cargo trafficking and synapse assembly. Adv Exp Med Biol 970:173–196
71. Xu C, Klaw MC et al (2015) Pharmacologically inhibiting kinesin-5 activity with monastrol promotes axonal regeneration following spinal cord injury. Exp Neurol 263:172–176
72. Yamazaki M, Miyazaki H et al (2002) Phosphatidylinositol 4-phosphate 5-kinase is essential for ROCK-mediated neurite remodeling. J Biol Chem 277(19):17226–17230
73. Yu X, Wen H et al (2013) Temporal and spatial expression of KIF3B after acute spinal cord injury in adult rats. J Mol Neurosci 49(2):387–394
74. Zacharova G, Sojka D et al (2009) Changes of parvalbumin expression in the spinal cord after peripheral inflammation. Physiol Res 58(3):435–442
75. Zai LJ, Wrathall JR (2005) Cell proliferation and replacement following contusive spinal cord injury. Glia 50(3):247–257